OPEN ACCESS
IOP Publishing
Journal of Physics G: Nuclear and Particle Physics
J. Phys. G: Nucl. Part. Phys. **51** (2024) 085202 (25pp)
https://doi.org/10.1088/1361-6471/ad4bf8

Development of a silicon drift detector array to search for keV-scale sterile neutrinos with the KATRIN experiment

D Siegmann[1,2], F Edzards[1,2], C Bruch[1,2], M Biassoni[3], M Carminati[4,5], M Descher[6,7], C Fiorini[4,5], C Forstner[1,2], A Gavin[8], M Gugiatti[4,5], R Hiller[6], D Hinz[6], T Houdy[9], A Huber[6], P King[4,5], P Lechner[10], S Lichter[6], D Mießner[10], A Nava[3,11], A Onillon[1], D C Radford[12], D Spreng[1,2], M Steidl[6], P Trigilio[13], K Urban[1,2], D Vénos[14], J Wolfb[7] and S Mertens[1,2]

[1] Technical University of Munich, TUM School of Natural Sciences, James-Franck-Str. 1 D-85748 Garching, Germany
[2] Max Planck Institute for Physics, Boltzmannstr. 8, D-85748 Garching, Germany
[3] Istituto Nazionale di Fisica Nucleare (INFN), Sezione di Milano-Bicocca, I-20133 Milano, Italy
[4] Istituto Nazionale di Fisica Nucleare (INFN), Sezione di Milano, I-20133 Milano, Italy
[5] DEIB, Politecnico di Milano, Via Golgi 40, I-20133 Milano, Italy
[6] IAP, Karlsruhe Institute of Technology, Hermann-von-Helmholtz-Platz 1, D-76344 Eggenstein-Leopoldshafen, Germany
[7] ETP, Karlsruhe Institute of Technology, Wolfgang-Gaede-Str. 1, D-76131 Karlsruhe, Germany
[8] University of North Carolina at Chapel Hill, 120 E. Cameron Avenue, Chapel Hill, 27599 NC, United States of America
[9] IJCLab, Université Paris-Saclay, 15 rue Georges Clémenceau, F-91405 Orsay cedex, France
[10] Halbleiterlabor der Max-Planck-Gesellschaft, Isarauenweg 1, D-85748 Garching, Germany
[11] University of Milano-Bicocca, Piazza della Scienza 3, I-20126 Milano, Italy
[12] Oak Ridge National Laboratory, 1 Bethel Valley Rd, Oak Ridge, TN 37830, United States of America
[13] XGLab SRL, Bruker Nano Analytics, Via Conte Rosso 23, I-20134 Milano, Italy
[14] Nuclear Physics Institute of the CAS, v. v. i., 250 68 Řež, Czech Republic

E-mail: daniel.siegmann@tum.de

Received 25 January 2024, revised 25 March 2024
Accepted for publication 15 May 2024
Published 19 June 2024

Abstract

Sterile neutrinos in the keV mass range present a viable candidate for dark matter. They can be detected through single β-decay, where they cause small spectral distortions. The Karlsruhe Tritium Neutrino (KATRIN) experiment aims to search for keV-scale sterile neutrinos with high sensitivity. To achieve this, the KATRIN beamline will be equipped with a novel multi-pixel silicon drift detector focal plane array named TRISTAN. In this study, we present the performance of a TRISTAN detector module, a component of the eventual 9-module system. Our investigation encompasses spectroscopic aspects such as noise performance, energy resolution, linearity, and stability.

Keywords: dark matter, sterile neutrino, silicon drift detector, KATRIN experiment, x-ray detector, electron detector

1. Introduction

Sterile neutrinos[15] are a natural and viable extension to the Standard Model of particle physics [1]. If their mass is in the keV range, they are a suitable dark matter candidate [1–4]. Depending on their production mechanism, they can act effectively as cold or warm dark matter. This can potentially help to mitigate tensions between predictions of pure cold dark matter scenarios and the observations of small scale structures in our Universe [5]. Indirect searches and cosmological observations set stringent limits on the active-sterile neutrino mixing amplitude of $10^{-6} > \sin^2\theta > 10^{-10}$ in a mass range of $1\,\text{keV} < m_4 < 50\,\text{keV}$ [6–10]. However, these limits are model-dependent and can be relaxed by several orders of magnitude by modifying the dark matter decay models [11]. Current laboratory limits on the mixing amplitude with values of $\sin^2\theta > 10^{-4}$ are orders of magnitude weaker compared to the cosmological limits [12–19].

One method to search for sterile neutrinos in a laboratory-based experiment is via their production in single β-decay. The electron-flavor neutrino emitted in the decay is a superposition of the neutrino mass eigenstates, including the keV-scale sterile neutrino. Correspondingly, the measured electron energy spectrum, shown in figure 1, is a superposition of the active and sterile neutrino decay branches. The experimental signature is a spectral distortion at energies $E \leqslant E_0 - m_4$, which includes a kink-like feature. Here, E_0 denotes the kinematic endpoint of the decay. A search based on single β-decay is sensitive to sterile neutrino masses of $m_4 \leqslant E_0$.

The Karlsruhe Tritium Neutrino (KATRIN) experiment is designed to measure the effective electron antineutrino mass with a sensitivity better than 300 meV, by performing a measurement of the tritium β-decay spectrum near its endpoint energy of $E_0 = 18.6\,\text{keV}$ [20, 21]. Recently, the first sub-eV limit on m_ν of 0.8 eV (90% CL) based on the first two high-activity tritium measurement campaigns has been published [22–24]. The neutrino mass program of KATRIN is foreseen to continue until the end of 2025. Subsequently, the collaboration plans to upgrade the beamline, in order to perform a keV-scale sterile neutrino search by investigating the entire tritium β-decay spectrum. Considering the high source activity of KATRIN (e11 Bq), it would be in principle possible to achieve a statistical

[15] In the following, the term *sterile neutrino* denotes an additional fourth mass eigenstate which is not purely sterile and can thus mix with the three active neutrinos.

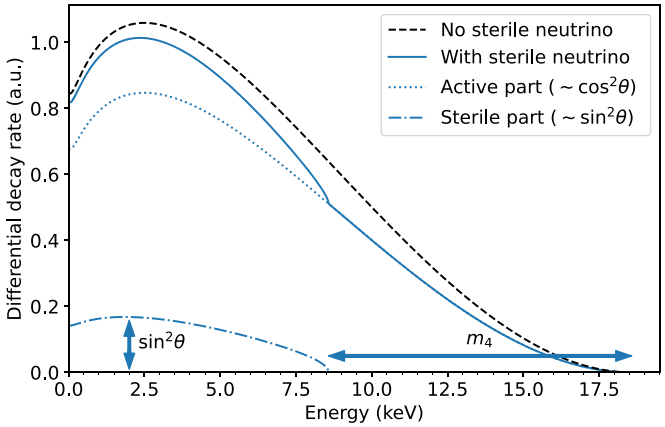

Figure 1. Electron energy spectrum of tritium β-decay shown with and without the imprint of a sterile neutrino. For illustrative purposes, a neutrino mass of $m_4 = 10$ keV and an unphysically large mixing amplitude of $\sin^2\theta = 0.2$ have been used.

sensitivity to keV-scale sterile neutrinos in the order of $\sin^2\theta < 10^{-8}$ within 3 years of data taking [25]. However, due to detector rate limitations and systematic uncertainties, the collaboration explores the possibility of reaching a sensitivity at the level of 10^{-6}.

As opposed to the neutrino mass measurements where the region of interest extends 40 eV below the endpoint energy E_0, the signature of a keV-scale sterile neutrino lies much further away from the endpoint, due to its unconstrained mass scale. By extending the measurement interval deeper into the tritium spectrum, the KATRIN experiment has the potential to search for sterile neutrino masses of $m_4 \leqslant E_0 \approx 18.6$ keV. Ultimately, the maximal accessible sterile neutrino mass range will depend on the beamline settings and adjustments which are subject of ongoing sensitivity studies that will be discussed in an upcoming publication. The current focal plane detector system [20, 21] is not designed to handle the associated exceedingly high count rates. To cope with this challenge, a new detector system, named TRISTAN, with more than 1000 pixels and a targeted energy resolution of 300 eV FWHM at 20 keV is currently being developed. It is based on the silicon drift detector (SDD) technology which provides excellent spectroscopic properties at the envisioned high rates of 100 kcps per pixel. Thanks to their small readout anode, and thus small detector capacitance in the order of 120 fF, SDDs feature an excellent energy resolution of 180 eV FWHM for 5.9 keV x-rays at short energy filter shaping times of 0.5 μs [26].

The TRISTAN detector system features a modular design. It consists of several identical detector modules that can be mounted next to each other as shown in figure 2. Each detector module has 166 pixels. In the baseline design, the detector system will be composed of 9 detector modules with a total of about 1500 pixels. In this configuration, the detector system can be installed in the beamline of the KATRIN experiment with only minor modifications of the current detector section. However, due to the circular shape of the beamline, some of the outer pixels of the detector system are covered and only about 1000 pixels can be illuminated. Due to the modular design of the detector system, a potential upgrade using 21 modules, is technologically feasible and could further improve the statistical sensitivity. However, due to the bigger dimensions, such an upgrade would require a redesign of the detector section.

The main goals of this work are the commissioning and the characterization of the first TRISTAN detector modules with photons and electrons. We present results obtained in

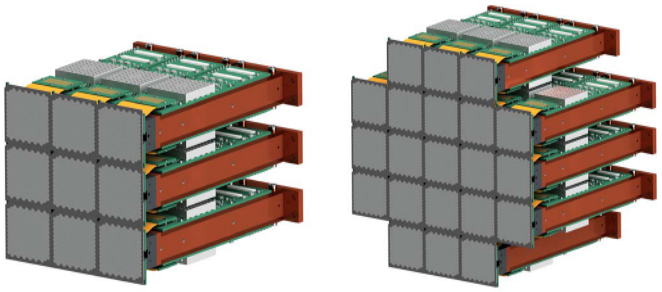

(a) Baseline (9 modules) (b) Upgrade (21 modules)

Figure 2. Renderings of the TRISTAN detector system consisting of 9 modules (baseline design) and a potential upgrade consisting of 21 modules.

dedicated test stands and the first operation of a detector module under quasi-realistic conditions (e.g. vacuum, electric and magnetic fields) in the KATRIN monitor spectrometer.

2. TRISTAN detector module

A photograph of a TRISTAN detector module is shown in figure 3. It consists of a large rectangular monolithic multi-pixel SDD chip which is glued on a silicon ceramic composite called Cesic. The SDD is electrically connected to the electronic readout boards via two rigid-flex printed circuit boards. All parts are mounted on the copper cooling structure. The requirements for the detector module and its individual components are explained in the following sections.

2.1. Detector module requirements

To cover the entire electron flux tube of the KATRIN experiment, a detector system with a diameter of approximately 20 cm is required. Even though the concept of the SDD is very flexible in terms of size and shape, building one large monolithic SDD chip with more than 1000 pixels is considered not to be technologically feasible. Therefore, the detector system has to be segmented into smaller detector modules. As shown in figure 3, the entire on-module electronics are placed in a plane perpendicular to the SDD chip, on two identical electronics readout boards. This arrangement allows for an almost seamless placement of the detector modules next to each other, see figure 2, minimizing the insensitive area of the detector system.

All components of the detector module have been selected carefully to ensure compatibility with the environment in the KATRIN experiment, that is based on the MAC-E filter (magnetic adiabatic collimation with an electrostatic filter) principle [20, 21, 27]. In particular, they need to be suited for high magnetic fields of up to 2.5 T [20, 21], and need to have a low outgassing rate since the detector chamber is connected to the MAC-E filter vessel, called main spectrometer. The dominant outgassing contribution of the TRISTAN detector system can be attributed to the material of the electronics PCBs (FR4) with a value of about 3×10^{-7} mbar L s^{-1} for each detector module [28]. Since the width of the electronics PCBs is limited by the SDD chip size, a high-density 12-layer design is necessary to accommodate all required connections. Due to the complexity of the electronics PCBs, no other low-outgassing material could be used. This includes for example the polyimide Kapton which is used for the

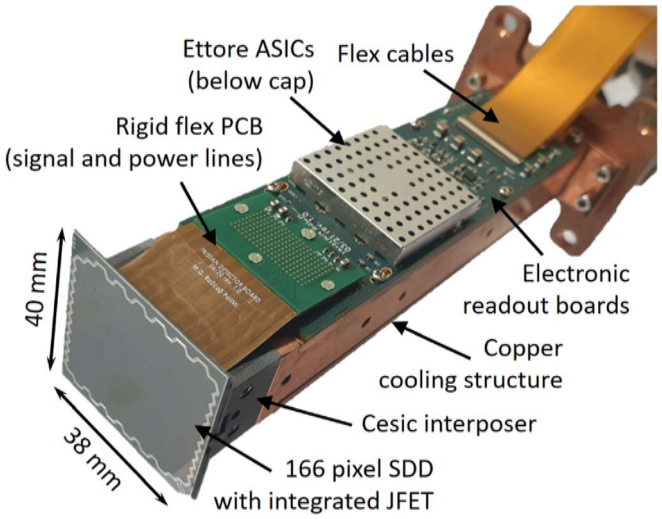

Figure 3. Photograph of a TRISTAN detector module. It consists of a monolithic 166 pixel SDD chip which is glued on a Cesic interposer. The interposer is connected to a copper cooling structure. The readout electronics boards with dedicated readout chips are mounted on the top and bottom surfaces of the copper block.

other electronic components. To compensate for the additional gas load stemming from the electronics PCBs, the conductance between the detector section and the main spectrometer has to be reduced. This is realized via a stainless steel grid which covers the gaps between the SDD chips. In addition, the pumping speed inside the detector section will be increased. As a reference, in the ongoing neutrino mass measurements, an ultra-high vacuum of 10^{-11} mbar in the main spectrometer is required to keep the background rate at a level of 220 mcps [24]. To achieve this pressure, the gas load stemming from the detector section needs to be on the order of 5×10^{-8} mbar L s^{-1} [28]. However, for the keV-scale sterile neutrino search with KATRIN, the requirements on the background are less stringent. The signal rate is up to eight orders of magnitude higher and therefore a vacuum pressure on the order of 10^{-9} mbar can be tolerated. First test measurements at this elevated pressure in the main spectrometer show indeed no significant increase of the background rate in the region of interest. However, in this measurement, a small increase of the background (less than 1 cps) at energies slightly below the retarding potential has been observed. The exact production mechanism of this background is currently under investigation.

2.2. SDD chip and readout electronics

The monolithic SDD chip consists of 166 hexagonal pixels. It is manufactured by the Semiconductor Laboratory (HLL) of the Max Planck Society from a silicon wafer with a thickness of about 450 μm. SDDs are semiconductor detectors that use the principle of sideward depletion [29, 30]. The detector bulk is depleted by applying a bias voltage to the entrance window side, i.e. the side on which the radiation enters the detector. Several drift rings on the opposite side, the readout side, form the electric field within the detector. As soon as radiation enters the detector, electron–hole pairs are created. The electrons are collected at a small anode (diameter of 82 μm) on the readout side. In order to minimize detector-related effects such as charge sharing, backscattering, and back-reflection, a pixel size with a

circumscribed diameter of 3.298 mm has been chosen [31]. The area of the hexagon corresponds to a circle with a diameter of 3 mm. The pixels are arranged in a gapless and continuous way, resulting in a sensitive area of about $37 \times 37\text{mm}^2$ and a total chip size of $38 \times 40\,\text{mm}^2$.

To take full advantage of the small anode with a detector capacitance of only 180 fF, an n-channel junction-gate field-effect transistor (nJFET) is directly integrated into each pixel. This configuration reduces the stray capacitance between the sensor and the charge sensitive amplifier (CSA) and makes it possible to place the readout electronics several centimeters away from the detector. The signals are amplified by a readout application-specific integrated circuit (ASIC) called ETTORE, that was specifically developed for the TRISTAN project [32]. Each ETTORE ASIC provides the amplification for up to 12 pixels. The connection between the detector and the readout electronics is realized via wire bonds that are connected to a partially flexible PCB (rigid flex PCB) that is mounted on the electronics board. The rigid flex cables allow for a 90° bent connection between the detector plane and the plane of the electronics boards. More details on the readout electronics of the TRISTAN detector module can be found in references [33–35].

2.3. Assembly procedure

In the following paragraphs, the different steps of the mounting procedure of the TRISTAN detector module will be described.

2.3.1. PEEK mounting jig. The SDD chip is very fragile, particularly on the entrance window side. For the detector assembly, a special mounting frame made from the thermoplastic polymer PEEK was designed. It supports the detector chip during the mounting procedure without touching any part of the entrance window.

2.3.2. SDD gluing. One of the most critical steps is the gluing of the SDD chip on the Cesic interposer. Cesic is a material that matches the coefficient of thermal expansion of the SDD and provides a solid mechanical interface to the copper cooling structure. Prior to the gluing, all parts involved in the assembly procedure are cleaned thoroughly. First, the two rigid flex cables are glued on the edges of the Cesic interposer using a two component, electrically insulating, thermally conductive epoxy (EPO-TEK-920FL [36]). After curing, small stripes of polyethylene terephthalate (PET) tape (thickness of190 μm) are attached to the outer edges of the large polished surface of the interposer. These PET stripes are used to ensure a defined glue thickness[16]. A thin layer of glue with a thickness comparable to the PET stripes is applied to the planar surface of the Cesic interposer as shown in figure 4(a). Afterwards, the SDD chip is placed inside the PEEK jig with the entrance window facing downwards, see figure 4(b). Finally, using an aligner, the Cesic interposer is positioned on top of the SDD chip as illustrated in figures 4(c) and (f). Curing is performed in an oven under nitrogen atmosphere at a temperature of 60 °C for about 5.5 h.

2.3.3. Wire bonding. In the next step, the detector is electrically connected to the readout electronics using ultrasonic wire bonding. In particular, 361 aluminum wire bonds with a diameter of 25 μm connect the readout side of the SDD chip with the two rigid flex cables, see

[16] In the first iteration of the procedure, a glue containing spherical spacer balls with a diameter of 70 μm was used to create a well defined spacing between the Cesic interposer and the detector. However, it turned out that the spacer balls damaged several detector pixels. As a result, the glue has been replaced and the PET stripes have been included in the assembly to better define the spacing.

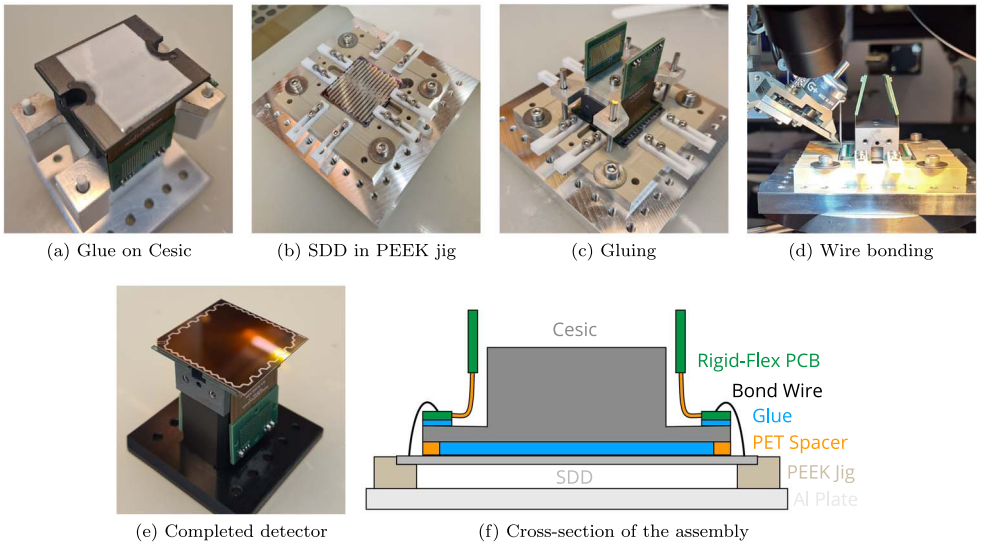

(a) Glue on Cesic (b) SDD in PEEK jig (c) Gluing (d) Wire bonding

(e) Completed detector (f) Cross-section of the assembly

Figure 4. Photographs and schematic of the detector module assembly procedure. (a) Cesic interposer with white glue just before the assembly on the SDD chip. (b) SDD chip with the readout side facing up in the PEEK jig. (c) Assembly of the Cesic interposer on top of the SDD. (d) Wire bonding of the SDD to the rigid-flex PCB. (e) Detector module after gluing and bonding. (f) Cross-section of all parts involved in the assembly of the detector module.

figure 4(d). Two additional bond wires from the rigid-flex PCB to the entrance window side are required for the depletion voltages of the SDD chip. To this end, one small corner of the SDD chip is cut away as can be seen in the photograph in figure 4(e).

2.3.4. Electronics assembly. In the last step, the Cesic interposer holding the SDD is screwed onto the copper cooling block. Thereupon, the two electronics PCBs, called ASIC boards, are mounted on each side of the copper block. The rigid flex cables are connected to the ASIC boards via dedicated Z-ray compression connectors. Finally, the ASIC boards are connected to the bias system and the data acquisition (DAQ) system using dedicated cables and feedthrough flanges.

3. Experimental setups

Three experimental setups were used to characterize the TRISTAN detector module: (1) a bench test setup for the characterization with x-rays, (2) a vacuum chamber with an electron gun for the characterization with electrons, and (3) the KATRIN monitor spectrometer. These setups will be discussed in more detail in the following sections.

In all setups, data has been acquired using three synchronized CAEN VX2740B digitizers. Each unit performs a full waveform digitization for up to 64 channels with a sampling rate of 125 MHz at a 16 bit resolution. A trapezoidal filter with an exponential baseline correction is applied to reconstruct the energy of the individual events [37]. If not stated otherwise, for the measurements performed in the scope of this work, an energy filter rise time of $t_{\mathrm{rise}} = 2\ \mu$s and a flat top time of $t_{\mathrm{top}} = 0.3\ \mu$s have been used.

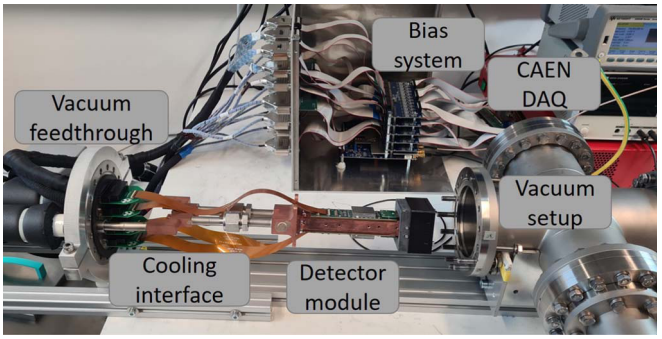

Figure 5. Photograph of the x-ray bench test setup. The detector module in the center of the photograph is protected by a cover which at the same time serves as a holding structure for calibration sources. The detector module and the readout electronics are connected to a cooling interface system. The test setup features a feedthrough for all electrical connections as well as for the cooling pipes. Inside the vacuum, the detector and readout electronics are connected via four Kapton flat cables. Outside the vacuum, the signal lines are connected to the bias system via twisted cable pairs. The connection of the signal lines to the DAQ system is realized using short flat cables.

Most of the measurements presented in the following have been performed with a TRISTAN detector module (internal nomenclature: S0-166-4) in the bench test setup and in the monitor spectrometer. To validate some of the results, a second detector module (S0-166-6) has been used for investigations in the electron gun vacuum chamber. The detectors used in this work are prototypes of the final module design.

3.1. X-ray bench test setup

In a first step, the TRISTAN detector module has been characterized with x-rays in a bench test setup at the Max Planck Institute for Physics, see figure 5. It consists of a vacuum- and light-tight tube-like vessel made from stainless steel and roughly resembles the geometry of the detector section in the KATRIN monitor spectrometer. The setup is assembled on rails such that the detector module can be accessed easily. The copper block on which the detector module is mounted is connected to a cooling system to operate it at a temperature of $-35\,^{\circ}\mathrm{C}$. A protective cover can be installed at the detector entrance window side to protect the sensitive area of the SDD and the wire bonds. At the same time, this cover can be used for the installation of a radioactive calibration source at a distance of about 12 mm to the SDD chip. For the detector module characterization with x-rays, ^{55}Fe and ^{241}Am sources were used. While the ^{55}Fe source features two prominent x-ray lines at energies of 5.9 keV ($\mathrm{Mn}-\mathrm{K}_{\alpha}$) and 6.4 keV ($\mathrm{Mn}-\mathrm{K}_{\beta}$), respectively, the ^{241}Am source has several monoenergetic x-ray, gamma ray and, fluorescence lines in the energy range 5–60 keV [38, 39]. Representative for the measurements in this work, figure 6 shows a typical pixel map of the measured count rate for ^{55}Fe events with energies above 1.5 keV. The threshold of 1.5 keV has been selected in the data acquisition system since the intrinsic threshold of the detection system with a value of about 1.4 keV varies slightly between pixels.

3.2. Electron gun vacuum chamber

The characterization of the detector module with electrons was performed using a customized electron gun installed in a cylindrical vacuum chamber [40], see figure 7. For the

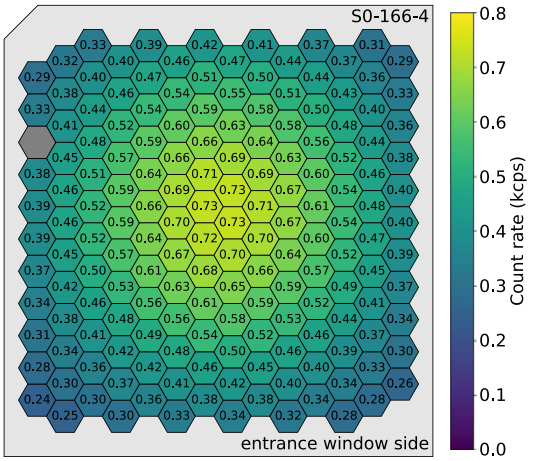

Figure 6. Typical pixel map showing the rate distribution measured with an ^{55}Fe calibration source in the x-ray bench test setup. The measured count rate for events with energies above 1.5 keV is represented by the color bar. The pixels are shown as seen from the entrance window side. The pixel marked in grey had to be disabled due to a loose contact in the signal line.

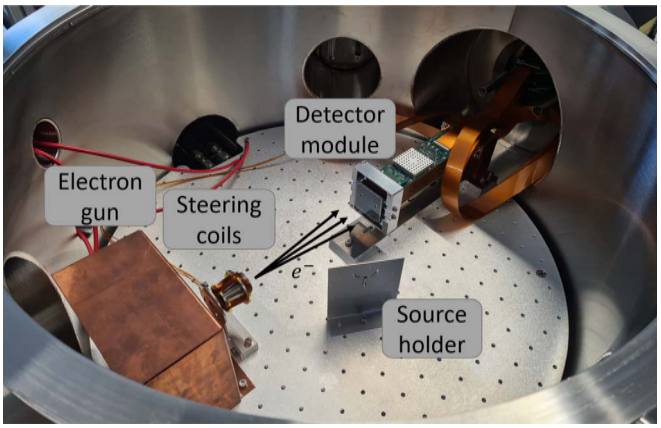

Figure 7. Photograph showing the electron gun vacuum chamber. The electron gun is based on a hot cathode using a tantalum wire. Electrons are accelerated via an electric field to energies up to 20 keV. They are guided via steering coils towards the entrance window of the detector. The detector module is mounted at a distance of about 25 cm to the electron source. Parts of the protection cover made from aluminium are still installed on the detector module. Several feedthroughs are used for cable routing, vacuum, and cooling.

measurements with electrons, good vacuum conditions are required since they have a small free streaming length in air. Using a turbo-molecular pump directly connected to the vacuum chamber, pressure levels as low as 10^{-7} mbar are achieved in the test setup.

The electron gun is based on a hot cathode made from a tantalum filament (wire diameter of 25 μm). By applying a voltage and thus heating the wire, electrons are emitted as soon as their thermal energy exceeds 4.3 eV (work function for tantalum) [41]. The filament is

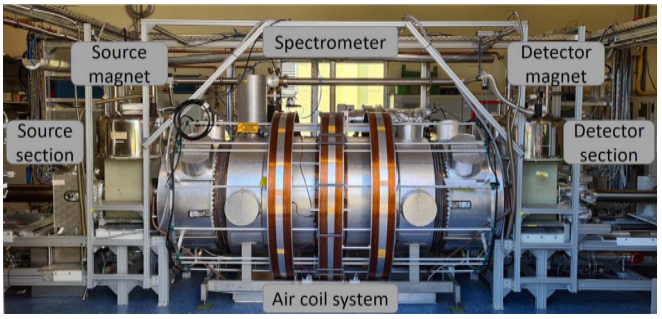

Figure 8. Photograph of the KATRIN monitor spectrometer. The spectrometer is shown in the center, while the two superconducting magnets can be seen on each side. The spectrometer is surrounded by three copper coils which shape the magnetic field inside the vessel. The evaporated ^{83m}Kr source is installed in the source section at a position close to the source magnet. The TRISTAN detector module is mounted in the detector section close to the detector magnet.

positioned such that there is no direct line of sight to the detector. This is necessary to minimize the leakage current caused by the emission of photons from the hot cathode. The electron rate can be set in the range 1–30 kcps by adjusting the wire temperature. The tantalum wire is mounted in a stainless steel cage which is connected to a high voltage power supply. By applying an electric field of up to 20 kV to the cage, electrons are accelerated towards the detector module. The beam illuminates roughly 10 pixels at once. Magnetic steering coils mounted in front of the electron gun are used to guide the electrons such that the entire entrance window surface of the detector is illuminated homogeneously [40].

3.3. KATRIN monitor spectrometer

In order to characterize the TRISTAN detector module in a more realistic environment (magnetic field, vacuum, high voltage, etc), it has been installed in the KATRIN monitor spectrometer. A photograph of the apparatus is shown in figure 8. The monitor spectrometer was initially used as a high voltage monitoring device for the KATRIN neutrino mass measurements. More recently, it has been repurposed as a test facility for potential hardware upgrades of the KATRIN experiment. The spectrometer as well as many other parts come from the former Mainz neutrino mass experiment, one of the predecessors of KATRIN [42]. The spectrometer is a stainless vessel with a diameter of 1 m and a length of about 3 m. Two superconducting magnets provide a strong magnetic field of up to 6 T on each side of the spectrometer [43]. The spectrometer vessel is surrounded by a system of air coils which shapes the magnetic field and compensates for the Earth magnetic field. A set of cylindrical and conical electrodes mounted inside the spectrometer allows fine adjustment of the electric fields.

The operating principle of the monitor spectrometer is based on the MAC-E filter principle which is also utilized in the KATRIN experiment [20, 21, 27]. Electrons created in a high magnetic field (3.6 T) in the source section are guided on a cyclotron motion along the magnetic field lines towards the spectrometer. Due to the reduction of the magnetic field strength towards the center of the spectrometer (3 mT), the transverse momentum of the electrons is adiabatically transformed into a longitudinal one. By applying a retarding voltage to the electrodes of the spectrometer, an electric field parallel to the magnetic field lines is created. This field acts as a high-pass filter to the longitudinal component of the electron

Table 1. Conversion electrons from the ^{83m}Kr source used for the experimental investigations (values corresponding to the 32.15 keV γ-decay). The weighted average of the L and M lines is calculated using the intensity per decay. Values taken from [45].

Line	Energy (eV)	Intensity per decay (%)	Weighted average (eV)
K	17824.2(5)	24.8(5)	
L_1	30226.8(9)	1.56(2)	
L_2	30419.5(5)	24.3(3)	
L_3	30472.2(5)	37.8(5)	30446.1
M_1	31858.7(6)	0.249(4)	
M_2	31929.3(5)	4.02(6)	
M_3	31936.9(5)	6.24(9)	
M_4	32056.4(5)	0.0628(9)	
M_5	32057.6(5)	0.0884(12)	31933.9

momentum. All electrons with a longitudinal momentum sufficient to overcome the retarding potential are magnetically guided to the TRISTAN detector in the detector section. At the position of the detector, the magnetic field has a value of 100 mT. In addition, a vacuum level of below 10^{-8} mbar at the detector position and 10^{-10} mbar in the spectrometer can be achieved.

To characterize the TRISTAN detector in the monitor spectrometer, three different types of x-ray and electron sources were used.

3.3.1. ^{55}Fe source. To investigate the detector system with x-rays, an ^{55}Fe calibration source was installed in the beamline of the monitor spectrometer inside the detector section. The source was moved in front of the detector using a movable source holder [44].

3.3.2. ^{83m}Kr source. The detector response to electrons was characterized using an ^{83m}Kr source evaporated on the surface of a highly oriented pyrolithic graphite (HOPG) substrate. It is installed in front of the superconducting solenoid on the source section side of the spectrometer. As listed in table 1, it provides quasi-monoenergetic conversion electrons in the energy range from 7 to 32 keV [45, 46]. In the scope of this work, internal conversion electrons of the gamma decay with an energy of 32.15 keV were used exclusively. For the energy calibration, a weighted average of corresponding sublines was calculated. This is required since the detector cannot resolve energetic separations on the eV scale. As an example, the L-32 electron line corresponds to the weighted average of the L_1, L_2, and L_3 lines. The electron energy E_{Kr} as measured with the detector for a given electron line energy E_{line} can be described by the equation

$$E_{\mathrm{Kr}} = E_{\mathrm{line}} + |e \cdot U_{\mathrm{sc}}| - |e \cdot U_{\mathrm{bias}}|. \tag{1}$$

Here, e denotes the elementary charge, and U_{sc} an additional source potential which was set to a value of -500 V to effectively increase the electron emission rate towards the detector. The quantity $U_{\mathrm{bias}} = -115$ V indicates the biasing potential on the entrance window side of the detector.

3.3.3. Wall electrons. Secondary electrons emitted from the inner spectrometer electrode surface were used as a second electron source. In the following, we will refer to them as wall electrons. These electrons are created by high-energetic particles such as muons which interact with the spectrometer material facing the vacuum side. The electrons leave the surface

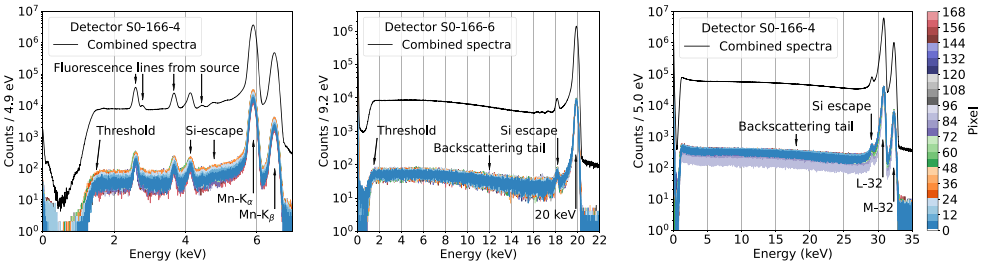

(a) ^{55}Fe spectrum (b) 20 keV electrons (c) L-32 and M-32 lines of ^{83m}Kr

Figure 9. Recorded energy spectra in the presence of x-ray and electron sources in the three different experimental setups. The black curve corresponds to the superposition of all energy spectra. The color bar indicates the individual pixels. (a) Measurement with an ^{55}Fe calibration source placed in front of the detector in the x-ray bench test setup. (b) Electron energy spectra measured with an electron gun at 20 keV in the vacuum chamber setup. In the combined spectrum, a small non-physical distortion can be observed at about 17 keV. It originates from an instability of the electron gun and is currently under investigation. (c) Energy spectra of the L-32 and M-32 lines in the presence of a ^{83m}Kr source in the monitor spectrometer. The source potential was set to $U_{sc} = -500$ V and the retarding potential to $U = 30.2$ keV.

with energies of $E_{sec} < 30$ eV (peak energy at $E_{sec} = 1$–2 eV) [47]. They are then accelerated in the direction of the detector via the potential U of the electrode system. The electron energy at the detector can be described by the equation

$$E_{wall} = E_{sec} + |e \cdot U| - |e \cdot U_{bias}|. \tag{2}$$

In the standard measurement configuration, the wall electrons are magnetically shielded from the spectrometer volume and are not detected [48]. In order to use these electrons for calibration and characterization purposes, the magnetic fields in the spectrometer can be intentionally adjusted such that they touch the walls. Consequently, the electrons are guided towards the detector. For the measurements performed in the scope of this work, wall electrons with energies from 10 to 32 keV and a total count rate of 25 cps were used.

4. Characterization of the TRISTAN detector modules

In this section, we present the results of the characterization of the TRISTAN detector with x-rays and electrons. In particular, properties such as the spectral response, the energy resolution, and the stability of the system will be discussed.

4.1. Detector response to x-rays

For the characterization of the detector response to x-rays, an ^{55}Fe calibration source was used. A typical energy spectrum recorded in the x-ray bench test setup is shown in figure 9(a). The $\mathrm{Mn} - \mathrm{K}_\alpha$ and $\mathrm{Mn} - \mathrm{K}_\beta$ lines at 5.9 keV and 6.5 keV, respectively, are clearly separated with an average energy resolution of 143.7 eV FWHM and 151.7 eV FWHM, respectively. Here, the energy resolution is extracted for each pixel and then averaged. In addition, the silicon escape peak corresponding to the $\mathrm{Mn} - \mathrm{K}_\alpha$ line can be seen. Here, the incident radiation ionizes an electron of the K-shell of the detector material. The created hole is filled by an electron from a higher-lying shell, emitting a photon with an energy of 1.74 keV [49]. This photon can be either reabsorbed by the detector or leave it undetected, leading to the